Experimental Characterization of a Reflective Amplified Modulator for Analog Applications

K.A. Mekonnen, J.H.C. van Zantvoort, E. Tangdiongga, A.M.J. Koonen

Institute for Photonic Integration, Eindhoven Univ. of Technology, Den Dolech 2, 5612AZ Eindhoven

We report on the analog characterization of a 35 GHz reflective electroabsorption modulator (REAM) monolithically integrated with a semiconductor optical amplifier (SOA). The device has a great potential as a low cost/consumption transmitter as it combines the high-speed modulation capabilities of a REAM with the amplification function of an SOA. Lossless operation over >40 nm range is measured. By optimizing the bias current of the SOA, higher modulation efficiency and larger operation range can be obtained. The dependence of the slope efficiency and radio frequency gain on REAM bias voltage, input optical power and SOA bias current are investigated.

Introduction

The radio-over-fiber (RoF) technology is a promising solution to transport broadband wireless data to radio access points (RAPs) [1]. It takes advantage of the excellent characteristics of single mode optical fiber such as low optical loss of < 0.2 dB/km, ultra-wide bandwidth, and no electromagnetic interference. The RAPs, where energy-, and cost-efficiency are strict requirements, perform optical-to-electrical and electrical-to-optical conversion in the downstream and upstream transmissions, respectively. Remotely controlled wavelength-agnostic reflective upstream transmitters (with centralized light sources) are preferred to implement simpler and more cost-efficient RAPs that can offer high-speed services.

Recently, the integrated semiconductor optical amplifier (SOA) and reflective electro-absorption modulator (REAM) as low-cost/energy-consumption upstream transmitter at remote sites has attracted much attention due to various benefits such as colorless operation, high bandwidth, small size, low driving voltage, potential for monolithic integration with other devices, and lossless operation [2–4]. It has a great potential as a low power consumption, low-cost and high bandwidth transmitter for both digital and analog communications, especially at RAPs. A continuous wavelength emitted by the central station is pre-amplified in the SOA, modulated and reflected by the REAM, and then boosted out by the SOA. For RoF applications, low driving voltage, large bandwidth, low optical insertion loss, radio frequency (RF) gain and dynamic range are critical parameters to characterize a transmitter [5].

In this paper, we investigate the insertion loss, slope efficiency and RF gain of a REAM-SOA in details. Results show that the SOA acts as a stabilizer for the REAM, resulting in similar performances for a range of input optical power levels and wavelengths, hence avoiding strict requirements of input power and wavelength control at the RAPs.

Device fabrication

Fig. 1 shows the zoomed photograph of the fabricated REAM-SOA. The device consists of a 400 μm long SOA monolithically integrated with a 70 μm long REAM. The SOA gain maximum was positively detuned from the REAM absorption age in order to obtain amplification in the EAM working spectral range using selective area growth technology in the metal-organic vapor phase epitaxy. The measured material gap wavelengths are

λ_{EAM} = 1453 nm and λ_{SOA}= 1523 nm. The gain spectrum shift gives rise to an enhanced performance allowing larger gain, modulation dynamics, and spectral ranges. The active structure is composed of AlGaInAs/InP based multiple-quantum wells (MQWs) between two InGaAsP separate confinement heterostructure layers. AlGaInAs/InP materials provide a better electron confinement compared to InGaAsP-based structures resulting in enhanced optical gain and quantum efficiency as well as higher bandwidth [4]. Single-regrowth semi-insulating buried heterostructure technology was implemented to obtain a reduced capacitance for the REAM. The contact separation between the REAM and the SOA was realized by proton implantation resulting in an inter-section resistance in the order of 1×10^6 Ω. The back and front facets were coated with high reflection coating anti-reflection coating, respectively. A tapered output waveguide tilted at 7° was realized to provide better coupling of the light to an optical fiber. The fabrication process is detailed in [3].

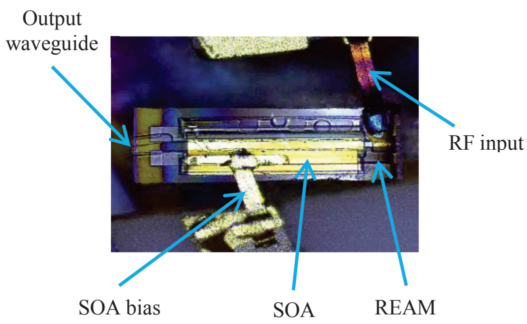

Fig.1 Photograph of the fabricated REAM-SOA device.

Device static characteristics

We first performed static characterization of the REAM-SOA. The device combines the amplification function of an SOA and high-speed operation capability of EAM on a single device. Fig. 2 depicts the insertion loss/gain of the device when the SOA was biased at 120 mA current and input optical power was 0 dBm for different wavelengths and EAM bias voltages. Lossless operation over a wavelength range of >40 nm was observed. For wavelengths between 1540 nm and 1560 nm an insertion gain >7.5 dB was measured. A small gain ripple is caused because of residual cavity feedback.

Fig. 3a shows the normalized fiber-to-fiber dc transfer curve for varying wavelengths at input optical power of 0 dBm and SOA bias current of 50 mA. We performed a 5th order polynomial fitting for the curves. The slope of the transmission curve decreased with increasing wavelength. Additionally, the optimum EAM bias shifted from -1 V to -1.5 V for wavelengths of 1530 nm to 1590 nm. The dependence of the dc transmission curve on SOA bias current and input optical power is also illustrated in Fig. 3b and Fig. 3c, respectively, for incident optical signal of wavelength 1550 nm. The slope decreased slightly with increasing SOA bias current and input optical power. On the other hand, improved linearity could be obtained with increasing SOA bias current and increased input optical power. This is because of the SOA gain saturation which provides a gain profile opposite to the REAM absorption profile. At lower input optical power levels and/or lower SOA bias currents, the device has slightly better modulation efficiency and higher insertion gain, and at higher input optical power and/or higher SOA bias currents, much improved linearity

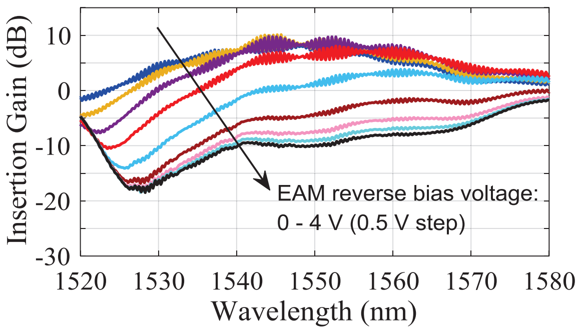

Fig. 2 REAM-SOA insertion gain vs wavelength of input optical signal with increasing EAM bias voltage

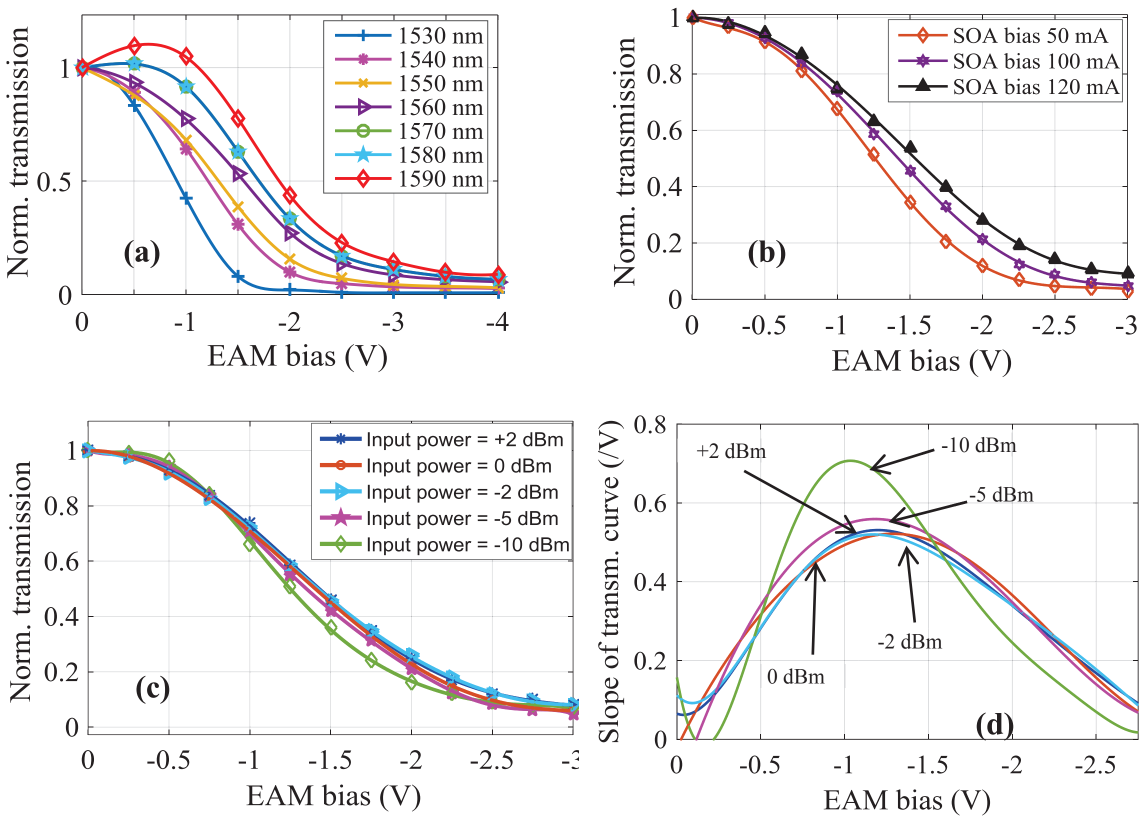

Fig. 3 Normalized fiber-to-fiber dc transfer curve: (a) for varying wavelengths at input optical power of 0 dBm and SOA bias current of 50 mA; (b) – (c) at varying SOA bias currents at input optical power of 0 dBm; and for varying input optical power at SOA bias current of 100 mA, respectively, for 1550 nm wavelength; (d) Slope of the transmission curve for input optical signal of 1550 nm at varying input optical power SOA bias current of 100 mA.

can be obtained, which can be useful for analog (or RoF) application, at slightly lower modulation efficiency. The bandwidth of the REAM-SOA was measured to be 35 GHz.

RF gain

RF gain, which depends on the modulation efficiency, is a very important parameter for characterizing an analog modulator. The modulation efficiency of analog modulators depends on the slope of the transmission curve [6]. Performance of EAMs with a MQW absorption region is very sensitive to the input optical power and wavelength [5, 6]. At low input powers, MQW EAMs have the maximum slope efficiency. With the increase of the input power, the slope decreases. Hence, careful control of the input signal is needed for EAMs. The presence of the SOA in the REAM-SOA balances this change in slope efficiency with opposite effect in the output power.

The slope of the transmission curve of the REAM-SOA, as obtained by taking the first derivative of the transfer curve with respect to the EAM bias voltage, is indicated in Fig. 3d for SOA bias current of 100 mA. The REAM-SOA showed the highest slope for input powers lower than -10 dBm. As the input optical power was increased, the slope showed negligible variation from 0.53 for a range of input optical powers, unlike regular EAMs [7]. The output optical power increased with increasing input optical power until it reached its saturation region. It only increased slightly when the input optical power was above -5 dBm. The combined effect was that the RF gain didn't vary by much for a range

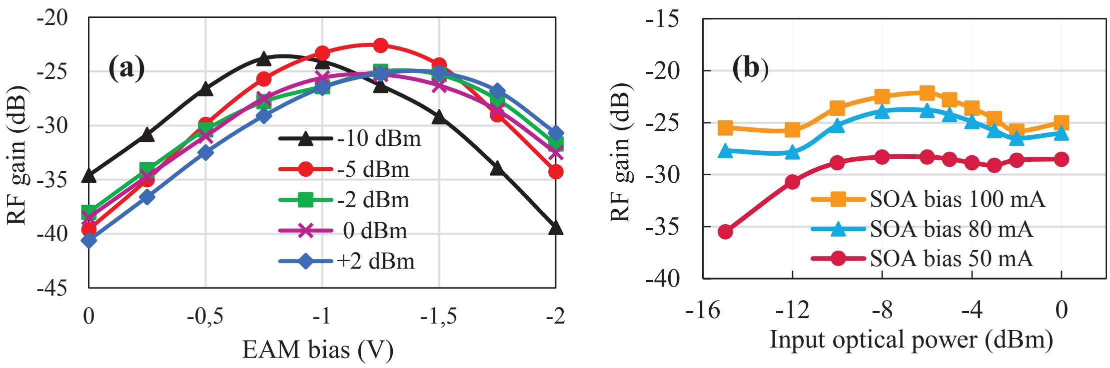

Fig. 4 REAM-SOA RF gain for input optical signal of wavelength of 1550 nm and RF input signal of 20 GHz frequency and -5 dBm power: (a) at varying input optical power and REAM bias voltage; (b) at varying SOA bias currents and input optical power.

of input optical power levels (see Fig. 4a). As shown in Fig. 4b, for a 20 GHz RF input signal with input power of -5 dBm, although the input optical power changed by 15 dB, the RF gain only varied by a maximum of 3 dB from the maximum which was obtained at input optical power of -6 dBm. The slope decreased with increasing SOA bias current. On the other hand, the output power of the device increased as the gain provided by the SOA increased with its bias current. The overall effect was an increase in the RF gain, which depends quadratically on the optical power. The maximum RF gain measured for a 20 GHz RF tone of input power -5 dBm was -22 dB, -24 dB, and -28 dB for SOA bias currents of 50 mA, 80 mA, and 100 mA, respectively which occurred when the input optical power was -6 dBm.

Conclusion

Characterization of a 35 GHz REAM-SOA, which combines the best features of an EAM and SOA on a single device, was presented for RoF applications. The analog performance stays largely unaffected by input signal optical power and wavelength as the SOA acts as a power stabilizer for the REAM. This alleviates the need for accurate control of the input signal, especially at RAPs, where simplicity and cost-efficiency are critical requirements.

This work was funded by the ERC as part of the Beam-steered Reconfigurable Optical Wireless System for Energy-efficient communication (BROWSE) project. We would like to thank the III–V Lab, Alcatel-Thales, France for providing the REAM-SOA chips.

References

[1] A. M. J. Koonen and E. Tangdiongga, “Photonic home area networks,” *J. Lightw. Technol*., vol. 32, no. 4, pp. 591, Feb. 2014.

[2] N. Dupuis et al., “10-Gb/s AlGaInAs colorless remote amplified modulator by selective area growth for wavelength agnostic networks,” *Photon. Technol. Lett*., vol. 20, no. 21, pp. 1808–1810, Nov. 2008.

[3] K. Lawnikzuk et al., “Reflective amplified modulator operating at 40 Gbps up to 85ºC as colorless transceiver for optical access networks,” in Proc. IPRM, pp. 116 – 119, Aug. 2012.

[4] M. Le Pallec, et al., “42 GHz bandwidth InGaAlAs/InP electro absorption modulator with sub-volt modulation drive capability in a 50 nm spectral range,” in Proc. IPRM, Jun. 2004, pp. 577–580.

[5] B. Liu et al., “Analog characterization of low-voltage MQW traveling-wave electroabsorption modulators,” *J. Lightw. Technol.*, vol. 21, no. 12, pp 3011 - 3019, Dec. 2003.

[6] J. Lim et al., “Analysis and characterization of traveling-wave electrode in electroabsorption modulator for radio-on-fiber application,” *J. Lightw. Technol*., vol. 21, no. 12, pp. 3004-3010, Dec. 2003.

[7] M. K. Chin et al., “Carrier screening of electric field and electroabsorption saturation in InGaAs-GaAs quantum well structure," *Electron. Lett.,* vol. 27, no. 25, pp. 2310-2312, Dec. 1991.